

A HYBRID SURFACE REFERENCE TECHNIQUE

R. Meneghini¹, J.A. Jones², T. Iguchi³, K. Okamoto⁴ and J. Kwiatkowski⁵

1. NASA/Goddard Space Flight Center, Greenbelt, MD 20771, U.S.
2. Science Systems and Applications, Inc. Lanham, MD, U.S.
3. National Institute of Information and Communications Technology, Tokyo, Japan
4. Osaka Prefecture University, Osaka, Japan
5. George Mason University, Fairfax, VA, U.S.

1. Introduction and Background

Measuring path attenuation at microwave frequencies along a satellite-earth or ground link dates back to the 1960's. Some of the first experiments that used these measurements to estimate characteristics of the rain include the work of Collis [1] and Harrold [2] among others where it was noted that path attenuation is closely related to path-averaged rain rate. It was also shown that the amount of scatter between the two quantities is particularly small at Ka-band frequencies (35 GHz) because both correspond approximately to the same moment of the drop size distribution [3]. Use of multi-wavelength forward scattering measurements in rain were reported by Furuhamra and Ihara [4] and Ihara and Furuhamra [5] who demonstrated that measurements over microwave links at two or more frequencies could be used to estimate parameters of the path-averaged drop size distribution. Measurements at millimeter wavelengths have also been performed to obtain data on path attenuation by light rain, drizzle and cloud water. More recent studies have employed path attenuation measurements at 25 and 37 GHz [6]. Despite measurement problems, a limited amount of data also has been collected at 8.75 GHz for vertical and horizontal polarizations. In principle, this type of measurement provides information on the mean particle shape which, in turn, can be related to the median mass or mass weighted diameter in a way similar to that used for ZDR methods.

A recent design study [7] focuses on combining measurements of path attenuation and backscattered power at two frequencies along a microwave link. This type of measurement would resemble the DPR (dual-frequency Precipitation Radar) measurement for the proposed GPM satellite in the sense that radar reflectivities and path attenuations can be combined to provide gate-by-gate estimates of the DSD parameters. The advantages of the link measurements are that the hydrometeors generally would be restricted to one type (rain or snow) and that the estimates of path attenuation should be significantly more accurate than the spaceborne radar estimates of this quantity. Consequently, the data

from the backscattering link may provide insight into the performance of dual-wavelength radar retrievals under nearly ideal circumstances.

Hitschfeld and Bordan [8] provided the fundamental work for radar measurements at attenuating wavelengths, showing that because of errors in the radar calibration constant and the $k-Z$ (specific attenuation- radar reflectivity factor) relationships, accurate attenuation correction becomes increasing difficult as the path attenuation increases. Their proposed solution was to measure the rain rate at some radar range r which serves to bound the errors in the rain rate estimates up to that range.

By using the surface as a reference target from which the attenuation could be estimated, it was shown [9] that the Hitschfeld-Bordan solution could be reformulated by using this path attenuation constraint to adjust either alpha ($k=\alpha Z^\beta$) or the radar constant. Using this surface reference technique (SRT), Marzoug and Amayenc [10] proposed an independent, final-value solution for the attenuation correction procedure. Kozu and Nakamura [11] proposed a DSD-based adjustment by fixing the N0 parameter and determining the effective mean diameter. Iguchi and Meneghini [12], in a survey of the various formulations and their relative merits, proposed a hybrid solution as a weighting between the Hitschfeld-Bordan and alpha-adjusted SRT. This was further generalized and applied to the TRMM PR data by Iguchi et al. [13]. Experimental tests of the method and modifications of the formulation have been presented in many studies.

2. Refinements in Surface Reference Technique

As noted in the introduction, an independent estimate of path attenuation is useful in constraining the solutions for the range-profiled rain rate particularly when the attenuation is large. Although the brightness temperature at microwave frequencies can supply this information, the SRT appears to be the only way to do this for a single-wavelength radar. (The mirror-image return has shown some promise but is restricted to near-nadir incidence over oceans at light to moderate rain rates.)

Corresponding author address: Robert Meneghini, NASA/GSFC, Code 975, Greenbelt, MD, U.S., 20771; email: bob@neptune.gsfc.nasa.gov

The basic idea of the SRT is to estimate the 2-way path attenuation as the difference between the normalized radar surface cross section outside and inside the rain. However, there are many ways to estimate the rain-free or reference value. One way is to compute the mean and variance of the rain-free surface cross section at each incidence angle over a fixed grid such as $1^{\circ} \times 1^{\circ}$ collected from repeated satellite overpasses (temporal average). A second way is to measure the mean and variance of the rain-free surface cross sections at each incidence angle over a moving window before the rain is encountered (along-track spatial reference). Alternatively, by noting that the rain-free cross section over the ocean can be accurately modeled by a quadratic function of incidence angle, such a fit using the rain-free cross sections within the scan serves as a reference curve (across-track spatial reference). A more sophisticated fitting procedure has been proposed by Li et al. [14] where the rain-free data are fit over the full domain to a model wind profile which provides, in turn, a reference surface from which to estimate path attenuation.

In the version 6 operational SRT algorithm (2a21) we have implemented a reference estimate that combines features of the along-track and across-track procedures. Because it uses features of both, we call it a hybrid SRT. At each cross-track scan, consisting of 49 fields of view over an angle range from -18° to 18° , we have available at each angle the sample mean and standard deviation of the last k rain-free surface cross sections. We next find the coefficients of the best-fit quadratic through these 49 mean values using a weighting function that is inversely proportional to the standard deviation of the along-track estimate at each FOV. The 2-way path attenuation at each raining field of view is then taken to be the difference between the (quadratic) reference curve and the apparent surface cross section.

The basic procedure is illustrated in the top panel of Fig. 1. Twice the standard deviation at each angle bin of the rain-free along-track reference data is represented by the length of the vertical bar (in black) where the mean rain-free value is at the center of the vertical bar. The quadratic fit through the data (with a weighting inversely proportional to the standard deviation) is represented by the blue curve. The values for a , b and c are given on the plot and represent values for the curve: $a + b\theta + c\theta^2$ where θ is the incidence angle in degrees. Note that the parameter b represents an asymmetry in the reference data between the right- and left-hand sides of the swath. Measurements of the apparent surface cross section within the swath are represented by the (red) diamonds. For the hybrid method the 2-way PIA at a particular angle is given as the distance between the quadratic curve and the diamond; for the along-track estimate, the 2-way PIA is taken to be the distance between the center point of the vertical bar and the apparent cross section at that angle.

If the data for this orbit are processed backward, the rain-free reference data change since the data will be taken as the rain-free values encountered just after the rain rather than just before the rain. Notice that the apparent cross sections (red diamonds) are the same in both cases since we are dealing with the same scan. The reference data, however, for the backward and forward processing differ. We can interpret the differences by noting that as the wind speed increases, the surface cross section decreases at near-nadir angles (less than 10°) and increases at off-nadir angles (greater than 10°). A comparison of the upper and lower figures shows that the reference data for the backward processing was taken from a region of lower wind speed than that from the forward processing. It is also worth noting that the data from the backward-processed region is more skewed (larger value of b) possibly indicating a larger gradient in wind speed (or a change in wind direction) between right- and left-hand sides of the swath.

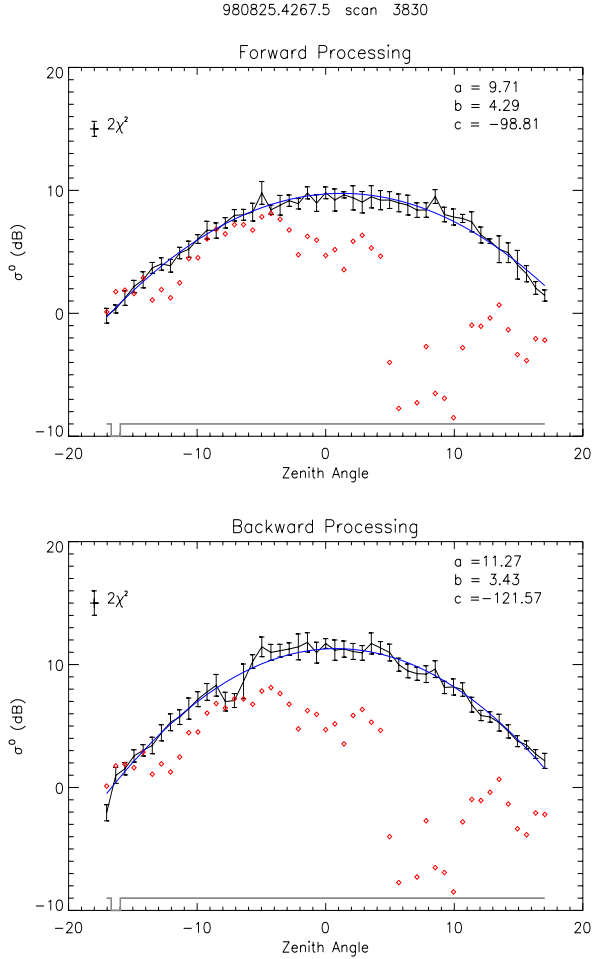


Fig. 1: Forward (top) and backward processing (bottom) of scan number 3830 over Hurricane Bonnie, (Aug. 25 1998 orbit 4267). Apparent surface cross sections are represented by the red diamonds. Vertical black bars represent the along-track reference data; blue curve represents the hybrid reference.

As suggested by this example, a comparison of the results from forward and backward processing provides information on the stability and reliability of the estimate. It also serves as a useful diagnostic tool and as a guide toward further improvements in the algorithm.

3. Tests of the Method

Recently the reprocessing of TRMM data using the version 6 algorithms has progressed through 1998. The reprocessing includes data from Hurricane Bonnie that was seen by the PR on 3 overpasses during the period of 24 – 26 August 1998. Because of the importance of accurate rain rate estimates in hurricanes and the dependence of the TRMM PR algorithms on the SRT, particularly for heavy rain rates, an examination of the SRT retrievals in Bonnie is instructive. This is especially true because the high and variable wind speeds near hurricanes implies that the reference data can change rapidly.

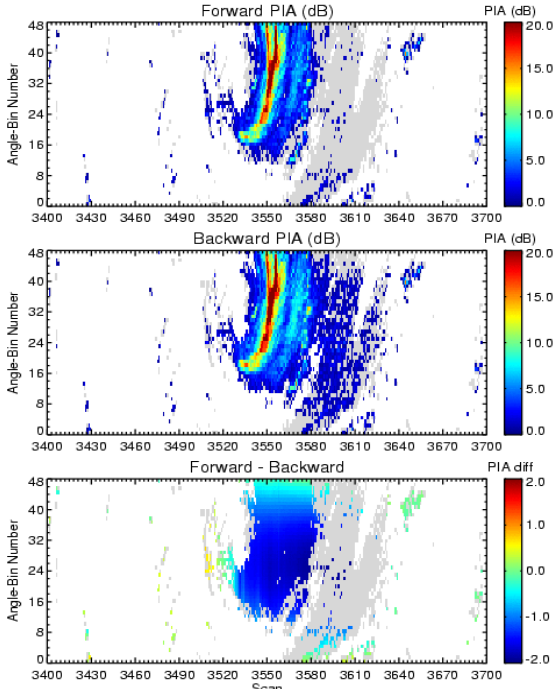


Fig. 2: Path-integrated attenuation estimates from a sequence of scans from orbit 4251 over hurricane Bonnie using forward (top) and backward processing (center). Difference between the path attenuations is shown in the bottom panel

Shown in Fig. 2 is that portion of orbit 4251 of 24 August 1998 over Bonnie displaying in the top panel the PIA from forward processing, in the center panel the PIA from backward processing and in the lower panel the difference between the two. The results show that at near-nadir angles the forward PIA is about 1-2 dB smaller than the backward PIA. At off-

nadir angles, the difference tends toward zero. As noted earlier, higher wind speeds are associated with lower near-nadir values of the NRCS, implying higher wind speeds for scan numbers less than about 3550 and higher for scan numbers greater than this. (Note that the grey areas in the upper two panels represent regions of rain where the PIA is negative; when either the forward or backward PIA is negative, the difference is not computed.)

The second PR overpass of Bonnie occurred on 25 August, orbit 4267 and is shown in Fig. 3 using the same conventions as in the previous example.

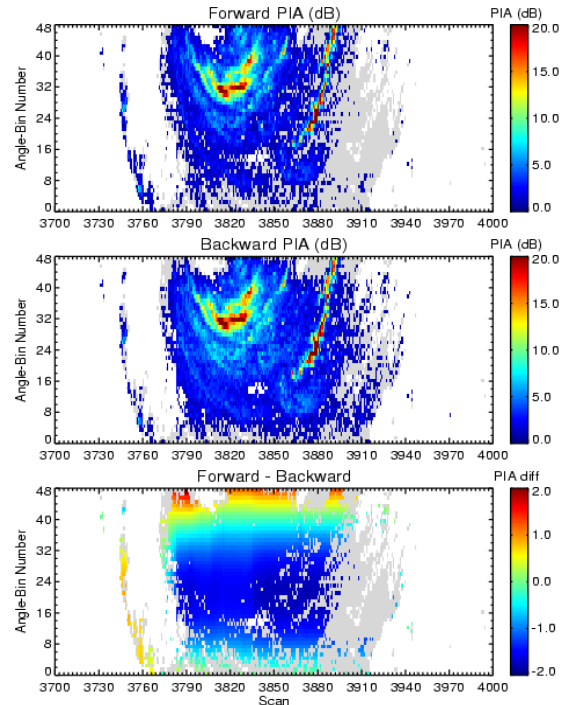


Fig. 3: Same format as figure 2 for segment of orbit 4267 on Aug. 25, 1998 over Bonnie.

The results are similar to the previous example in that the forward processed PIAs are smaller for the near-nadir angles (implying larger wind speeds at the lower scan numbers). Unlike the previous case, there is a clear sign reversal at the high incidence angles where the forward PIA is larger than the backward.

Fig. 4 shows results from the final overpass of Bonnie on Aug. 26. In this example we see a reversal from the previous two cases where the forward processing at near-nadir angles is now clearly larger than the backward processing. In the region centered near scan 5000 an even larger difference (~2 dB) is apparent. That this is related to the influence of the land is supported by the results in the bottom panel of Fig. 5 on which is plotted the surface cross sections along the swath and the abrupt change in the surface scattering properties in transitioning from land to

ocean. In this case, rain-free ocean reference data are either unavailable or insufficient for the forward processing so that the ocean reference data are taken far from the storm. In cases such as this, it is clear that the backward processing is the more appropriate reference for rain over ocean while the forward processed reference data is the more appropriate reference for rain over land.

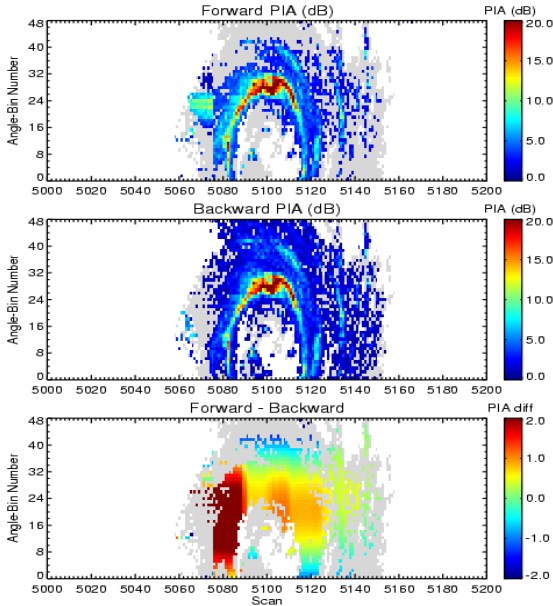


Fig. 4: Same format as Fig. 2 for orbit 4285 measured by the TRMM PR on August 26, 1998.

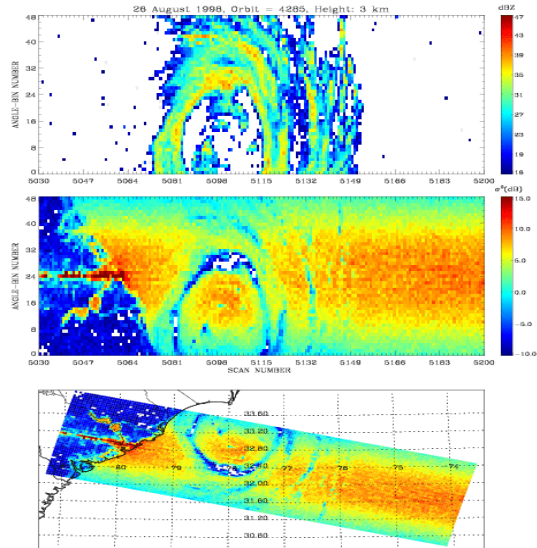


Fig. 5: Same scans as in Fig. 4 showing the radar reflectivity factor at 5 km (top) and the normalized radar cross sections (NRCS) of the surface (center). The bottom plot displays the NRCS with a map of the Carolina shore on the East coast of the U.S.

4. Discussion and Summary

Statistics from two weeks of PR data indicate that the use of the hybrid surface reference technique gives fairly consistent results. In particular, 75% of the reliable and marginally reliable data over ocean (about 60% of the oceanic rain data) give path-integrated attenuations from forward and backward processing that differ by less than 0.5 dB. Moreover, 90% of the differences are less than 1 dB [15].

Nevertheless, the examples shown here indicate that further improvements in the algorithm are needed. Since the operational algorithm uses only forward processing of the data, the addition of backward processing is desirable. This information should improve the accuracy of the PIA and aid in understanding the reliability and consistency of the estimates. The data should also provide more accurate estimates of path attenuation near coastlines where a forward or backward estimate alone is often insufficient. In situations such as hurricanes and typhoons where the wind speed and direction can change rapidly, the challenge will be to obtain an estimate from the two reference data sets that accurately represents the surface cross section beneath the rain.

References

- [1] Collis, R.T.H., 1961: Proc. 9th Wea. Radar Conf., 371.
- [2] Harrold, T.W., 1967, Proc. IEE London, **114**, 201-203.
- [3] Atlas, D. and C.W. Ulbrich, 1977, J. Appl. Meteor., **16**, 1322-1331.
- [4] Furuhama, Y.T. and T. Ihara, 1981, IEEE Trans. Ant. and Propag. **AP-29**, 275-281.
- [5] Ihara, T., and Y.T. Furuhama, 1984, Trans. IECE Japan, **E67**, 211-217.
- [6] Rincon, R.F. and R.H. Lang, 2002: IEEE TGARS, **GE-40**, 760-770.
- [7] Rincon, R.F. R.H. Lang and R. Meneghini, 2004: IGARSS04.
- [8] Hitschfeld W. and J. Bordan, 1954, J. Meteor., **11**, 58-67.
- [9] Meneghini, R., J. Eckerman, and D. Atlas, 1983, IEEE Trans. Geosci Remote Sens., **GE-21**, 34-43.
- [10] Marzoug, M. and P. Amayenc, 1994: J. Atmos. Oceanic Technol., **11**, 1480-1506.
- [11] Kozu, T. and K. Nakamura, 1991: J. Atmos. Oceanic Technol., **8**, 259-270.
- [12] Iguchi, T. and R. Meneghini, 1994: J. Atmos. Oceanic Technol., **11**, 1507-1516.
- [13] Iguchi, T., T. Kozu, R. Meneghini, J. Awaka, and K. Okamoto, 2000, J. Appl. Meteor., 2038-2052.
- [14] Li, L., E. Im, S.L. Durden, and Z.S. Haddad, 2002, J. Atmos. Oceanic Technol., **19**, 658-672.
- [15] Meneghini, R., J.A. Jones, T. Iguchi, K. Okamoto, and J. Kwiatkowski, 2004: J. Atmos. Oceanic Technol. (in press).